

**Advanced maternal age perturbs mouse embryo development and alters the
phenotype of derived embryonic stem cells**

Pooja Khurana¹, Neil R. Smyth¹, Bhavwanti Sheth¹, Miguel A. Velazquez², Judith J. Eckert³ and
Tom P. Fleming^{1,*}

¹*Biological Sciences, University of Southampton, Southampton General Hospital, Southampton
SO16 6YD, UK.*

²*School of Natural and Environmental Sciences, Newcastle University, Newcastle Upon Tyne
NE1 7RU, UK*

³*Human Development and Health, Faculty of Medicine, University of Southampton,
Southampton General Hospital, Southampton SO16 6YD, UK*

*Correspondence address. Tel: +44-2381-204145; E-mail: t.p.fleming@soton.ac.uk

Short title: Advanced maternal age alters stem cells

Abstract

Advanced maternal age (AMA) is known to reduce fertility, increase aneuploidy in oocytes and early embryos and lead to adverse developmental consequences which may associate with offspring lifetime health risks. However, investigating underlying effects of AMA on embryo developmental potential are confounded by the inherent senescence present in maternal body systems further affecting reproductive success. Here, we describe a new model for analysis of early developmental mechanisms underlying AMA by the derivation and characterization of mouse embryonic stem cell (mESC-like) lines from naturally-conceived embryos. Young (7-8 weeks) and Old (7-8 months) C57BL/6 female mice were mated with young males. Preimplantation embryos from Old dams displayed developmental retardation in blastocyst morphogenesis. mESC lines established from these blastocysts using conventional techniques revealed differences in genetic, cellular and molecular criteria conserved over several passages in standardised medium. mESCs from embryos from AMA dams displayed increased incidence of aneuploidy following Giemsa karyotyping compared with those from Young dams. Moreover, AMA caused an altered pattern of expression of pluripotency markers (*Sox2*, OCT4) in mESCs. AMA further diminished mESC survival and proliferation and reduced the expression of cell proliferation marker, Ki-67. These changes coincided with altered expression of the epigenetic marker, *Dnmt3a* and other developmental regulators in a sex-dependent manner. Collectively, our data demonstrate the feasibility to utilise mESCs to reveal developmental mechanisms underlying AMA in the absence of maternal senescence and with reduced animal use.

Key words: Advanced maternal age; mouse embryonic stem cells; blastocyst

Introduction

Whilst there is a global trend for women to delay bearing children, several studies indicate that advanced maternal age (AMA) leads to reduced ovarian reserve and infertility¹ and increased risk of pregnancy complications including gestational diabetes², preterm birth, hypertension and pre-eclampsia³⁻⁵. Moreover, AMA has been shown to adversely affect human offspring cardiometabolic and mental health^{6,7}.

The loss of ovarian reserve with AMA is common in mammals and may coincide with increased aneuploidy due to a range of segregation errors during meiosis affecting spindle dynamics⁸⁻¹⁰. However, maternal senescence also affects physiological condition across cell types and organs; for example, uterine decidualisation is diminished by AMA in human and mouse, affecting placental activity and increasing pregnancy loss^{11,12}. Moreover, senescence from AMA may promote a chronic maternal immune response affecting diverse fetal organ function and health¹³.

Given the confounding influence of maternal systemic senescence on AMA pregnancy success, models are required to understand the developmental potential of AMA oocytes and embryos and whether influenced or not by the extent and character of meiotic aneuploidy. Human and mouse embryos show retarded development in AMA^{14,15}. Moreover, where AMA blastocysts are transferred to young dams, offspring growth and cardiometabolic health are adversely affected¹⁵, indicating inherent compromised potential independent of maternal senescence and thereby demonstrating AMA contributes to the concept of the Developmental

Origins of Health and Disease (DOHaD) concept ¹⁶. This is supported by an altered transcriptome and signalling network expression detected in AMA human blastocysts ¹⁷.

In the current study, we assess the effect of AMA on mouse blastocyst development and establish a mouse embryonic stem cell (mESC) model for investigating AMA effects on incidence of aneuploidy and developmental potential. We believe this to be the first characterisation of mESCs directly from unstimulated naturally-conceived aged embryos although pluripotent stem cells have been generated from aged mouse artificially-activated oocytes forming parthenogenetic embryos (pES cells) ¹⁸. Also, mESCs have been generated from an assisted reproductive treatment (ART) model using mothers at different ages subjected to a combination of ART processes (maternal superovulation, *in vitro* fertilisation [IVF], extended culture to blastocyst) ¹⁹. We find AMA mESCs display a range of aneuploidic states and accompanying perturbation in cellular and expression characteristics that permit their exploitation for underlying mechanisms influencing development within the DOHaD context. To support these primary outcomes from ageing using male mESCs, we also include separate analysis of a secondary question, to assess differences in male versus female lines following ageing.

Methods

Animal procedures

Animal procedures were conducted under UK Home Office project license in accordance with Animal (Scientific Procedures) Act 1986 and local ethics committee at the University of

Southampton (UoS). We used Young (7-8 weeks) and Old (7-8 months) C57BL/6 females (UoS Biomedical Research Facility) to investigate AMA and these were naturally mated with sexually mature CBA males (10-15 weeks, Charles River Lab, UK). This protocol permitted consistency with our previous mouse AMA study showing AMA induced postnatal health changes¹⁵ and the cross combined the efficiency of C57BL/6 inbred strain for derivation of ESCs with increased hybrid vigour to generate genetically identical embryos with improved stability, as shown previously²⁰. Animals were housed on a controlled 07:00-19:00 h light cycle at 21°C and fed standard laboratory chow (Special Diet Services, Essex, UK) and water *ad libitum*.

Embryo collection and developmental staging

The morning after mating, dams were checked for a copulation plug to confirm successful mating. Midday on day after mating was classified as E0.5. At E3.5, C57BL/6 females were culled by cervical dislocation; dissected uterine horns were immediately placed in pre-warmed saline solution (BR0053G, Oxoid, UK) and the embryos flushed out in warm H6 medium supplemented with 4 mg/ml bovine serum albumin (BSA, Sigma, A3311)²¹. Collected embryos were transferred to fresh dishes containing 30 µl embryo culture medium, KSOM (Potassium supplemented simplex optimized medium) with amino acids²², and washed three times in these drops covered with a layer of mineral oil (Sigma Aldrich).

To evaluate effect of AMA on *in vivo* development, embryos derived from ten Young and Old dams were staged for development up to blastocyst and extent of blastocyst cavity

expansion (early, mid or late blastocysts). Mid-expanded blastocysts were washed in H6-BSA and used for embryonic stem cell (mESC) derivation.

Derivation and culture of mESC clones from E3.5 blastocysts

Mid-expanded blastocysts were transferred to freshly-prepared mouse embryonic fibroblasts (MEFs), mitotically inactivated with 10 µg/ ml mitomycin-C (MMC, Fisher Scientific, 10182953) in mESC medium [knockout-DMEM supplemented with 15% knockout serum replacement (KO/SR) (Gibco, 10828), non-essential amino acids (Gibco, 11140), 1 mM sodium pyruvate (Gibco, 11360), 100 µM 2-mercaptoethanol (Sigma, M7522), 2 mM glutamine, penicillin (50 U/ml)/ streptomycin (50 µg/ml) (Gibco, 10378) and 1000 U/ml of leukemia inhibitory factor (LIF)], and incubated undisturbed for 48 h under standard humidified conditions of 37°C in 5% CO₂ in air.

Blastocysts from different dams were plated onto different dishes where each blastocyst gave rise to an individual stem cell line. A total of 90 mid-stage blastocysts were utilized to derive 38 mESC lines. By the fourth day post plating of blastocysts from same dam on a single plate, inner cell mass (ICM) outgrowths could be observed to be hatched from the zona pellucida and attached on the MEFs. ICM clumps were enzymatically isolated using trypsin: ethylenediaminetetraacetic acid (EDTA) (0.05%; Gibco, 25300). Each isolated ICM outgrowth was collected in a different well of a 96-well U-shaped plate containing 50 µl/ well pre-warmed trypsin-EDTA, followed by careful pipetting up and down to achieve a single cell suspension. Trypsinized outgrowths were transferred to fresh flat-bottom 96-well MMC-MEF

coated plates and mESC medium was changed daily. Round, tight clusters of cells marked the first appearance of mESC clones, typically 4-5 days after plating the cells. Mouse ES colonies were cultured in mESC medium, passaged every 3-4 days by enzymatic dissociation and transferred to dishes with greater surface area when reaching 70% confluency. Once mESCs were expanded for 8-9 passages (P8-9; over 25-30 days), cells were either used directly or frozen at 1×10^6 cells/ cryovial in mESC medium with 20% KO/SR and 10% dimethyl sulfoxide, DMSO (Sigma, D5879). mESCs and MEFs were always counted and seeded in fixed proportions for each cell line and the cell numbers were kept consistent for individual experiments.

Sex analysis of derived mESC lines

MEFs were eliminated from the mESC co-culture by pre-plating on gelatin-coated dishes where they attached. After culturing the ES cells MEF-free, confluent mESCs were pelleted and treated with lysis buffer (10 mM Tris pH 8, 100 mM NaCl, 10 mM EDTA, 0.5% sodium dodecyl sulphate (SDS) and 1 mg/ml proteinase K) and processed with NaCl followed by isopropanol²³. Male and female mouse tail samples were used as controls. Genomic DNA concentration and quality was quantified using the Nanodrop ND-100 spectrophotometer. For sex analysis, genes *Sry* and *Zfy*, and *DxNds3* (or *Nds3*), located in the sex-determining regions of the Y- and X-chromosome respectively, were amplified by multiplex PCR. Amplified PCR products were run on agarose gels and bands were observed at 617 bp for *Zfy*, 404 bp for *Sry* and 244 bp for *DXNds3*. Within the Young group, 11 dams produced a total of 28 embryos that gave rise to 10 mESC lines, of which only 1 was female. Whereas, within the Old group, 13 dams produced a

total of 62 embryos resulting in 28 mESC lines with 4 being female. The male bias in sex ratio is in line with other mESC derivation studies because DNA methylation is globally reduced in XX mouse ESC lines and consequently may provide the basis for X-chromosome instability²⁴. Given that the Young group generated only one female mESC line, effects of maternal age were evaluated only between male mESC lines. However, as DOHaD animal studies often display sexually dimorphic data¹⁵, sex comparisons were also made within the Old group.

Chromosome counting (karyotyping) of mESC lines

70% confluent mESCs (P9-11) were harvested and treated with colcemid (0.1 µg/ml; Gibco, 15212-012) and incubated for 3 h at 37°C and 5% CO₂²⁵. Cells were washed, trypsinized, treated with KCl (75 mM, hypotonic solution) and fixed in the fixative solution (methanol: glacial acetic acid 3:1) before producing chromosome spreads. Slides were incubated with Giemsa stain (1:25 dilution; Sigma, G500) and analysed under a phase contrast microscope at x 100 magnification. Using Image J software, about 70 chromosome spreads were counted from each mESC line. Spreads were categorised as euploid ($2x = 40$), aneuploid ($2x \neq 40$), or polyploid ($2x \geq 80$). However, in accordance with the guidelines of American Type Cell Culture (ATCC), only karyotypically normal (>50% euploidy) mESC lines were used for further analysis. For chromosome analysis, six cell lines were screened each for Young and Old Male mESCs, as well as the Old Female mESC group.

mESC proliferation and viability assay

Established mESC lines (30,000 cells/ well; P9-11) were cultivated, harvested and seeded onto freshly prepared MMC-MEFs (27,000 cells/well) on 24-well plates in triplicates and cell counts performed at 24 h intervals up to 96 h. For counting unattached or dead cells, spent media were collected and centrifuged. Cells were counted using a Neubauer haemocytometer with viable cells detected by trypan blue (Sigma, T8154) dye exclusion assay. The mean number of cells per well was calculated at each assay time point.

Quantitative PCR (qPCR) analysis

mESCs (400,000 cells/well) were seeded on MMC-MEFs (135,000 cells/well) coated 6-well plates, cultured for 3-4 days, trypsinised and pre-plated to eliminate MEFs. RNA quality was preserved by gently mixing the derived pellet with RNA Later (Sigma, R0901). Total RNA was isolated using the RNeasy mini kit (Qiagen, UK) and quantified using the Nanodrop ND-1000 spectrophotometer. RNA integrity was analysed by the presence of clear 28S and 18S rRNA bands (in 2:1 ratio) by gel electrophoresis. First-strand cDNA was synthesized with 400 ng RNA using GoScriptTM Reverse Transcription System (Promega, UK) in the DNA Engine[®] Peltier Thermal Cycler (BioRad, UK). The primer-templates were annealed at 25°C for 5 min, extended at 42°C for 1 h and reverse transcriptase was inactivated at 70°C for 15 min.

Primers used for specific gene targets were from Primerdesign, UK ([Supplementary Table S1](#)) and were detected using the SYBR-green 2x PrecisionPlusTM Mastermix (Primerdesign, UK) protocol. Product was amplified using Chromo4 Real-time Detector

(BioRad, UK) and analysed with Opticon Monitor v3.1 software. The amplification program included enzyme activation at 95°C for 2 min, followed by 40 cycles of denaturation at 95°C for 10 s, annealing (and data collection) at 60°C for 1 min, and a final extension step at 72°C for 10 min. Melting curves were generated to confirm target-specific amplification by fluorescence detection between 60°C and 95°C at 1°C steps, holding for 15 s before the program was terminated. Target genes were normalised to stable house-keeping genes ²⁶ using Primerdesign geNorm kit ²⁷. Gene stability was determined using qbase+ software and genes *Ywhaz* and *Rpl13a* were identified as the most stable reference genes. Negative RT and water controls did not show amplification in the quantitation graphs. PCR products and primers were qualitatively analysed by gel electrophoresis and showed single bands at correct amplicon size.

Flow cytometry

Data acquisition was performed on FACSCalibur flow cytometer (BD Biosciences) and analyzed by FlowJo v.10 software. Fluorescence-activated cell sorting (FACS) was used to analyze the protein expression of (i) pluripotency (OCT4, NANOG and SOX2), (ii) proliferation (Ki-67), and (iii) apoptosis (Annexin V) and cell death (propidium iodide, PI) markers (antibodies used are listed in [Supplementary Table S2](#)) in undifferentiated mESCs (P9-P10) seeded on MMC-MEFs (135,000 cells/ well of a 6-well dish). In addition to using mESC-specific markers, MEF cells were further eliminated by adjusting the forward scatter (FSC, indicating cell size) and side scatter (SSC, indicating cell granularity) plots. While pluripotency analysis was conducted after culturing mESCs (200,000 cells/well) for three days; samples for cell proliferation (mESCs seeded at 150,000 cells/well) were collected every 24 h for 96 h. Cells

were stained for intracellular (nuclear) markers using Foxp3 Fixation/ Permeabilization working solution (Thermo Fisher Scientific, UK). For analysis, samples were re-suspended in flow cytometry staining buffer (PBS with 3% fetal bovine serum, FBS). Samples for cell apoptosis were prepared following eBiosciences AnnexinV-FITC Apoptosis kit protocol (BMS500FI) and mESCs (100,000 cells/well) were harvested every 24 h for 96 h. Anti-tumour agent etoposide (20 µg/ml, incubated for 4 h) induced apoptosis in Annexin V+ control samples, while floating cells were used as positive control for dead cells (PI+). The percentage of apoptotic cells was determined by generating a dual-colour dot plot (Annexin V-FITC (FL-1) vs. PI (FL-2)) and then setting a quadrant marker based on unstained and single-labelled control samples. The percentage of cells in each population and gate of interest were quantified for 20,000 cell events.

Immunocytochemistry

mESCs (30,000 cells/ well) were cultured on MMC-MEFs (27,000 cells/ well) (on sterile coverslips) in 24-well plates. At 70% confluency (3 days in culture), cells were fixed with 4% paraformaldehyde (PFA) and permeabilized in 0.2% Triton X-100 in PBS at room temperature. Non-specific antibody binding was blocked with 3% BSA and cells were stained with primary antibody at 4°C overnight. Cells were incubated with appropriate Alexa-Fluor conjugated secondary antibody in the blocking solution, for 1 h at room temperature ([Supplementary Table S2](#)). Cell nuclei were counterstained with DAPI pre-diluted in Mowiol mounting media. Images were captured using a Leica DM5000 B fluorescence microscope coupled to a Leica DFC300FX camera.

Statistics

For experimental analyses, four mESC lines derived from different blastocysts were used for AMA and control treatments. All lines were derived from separate mothers except two lines from Young male and Old female treatments which were from the same dam. Statistical analysis was performed using Statistical Package for the Social Sciences (i.e. IBM SPSS Statistics 24) with mother as a random variable for relevant sections comprising pluripotency expression, cell proliferation assays, cell death and apoptosis assays and qPCR assays. SPSS analysis showed dam origin had no significant effect. An independent Student's t-test was also used for embryo development, mESC derivation efficiency, sex differences and karyotype aberrations. Pairwise comparisons were made between Young male v Old male for effect of AMA on male embryo derived mESCs, and between Old male v Old female for effect of sexual dimorphism within the Old group with outcomes from both separate comparisons integrated into the same graphs for conciseness. Data were tested for assumptions of normality using the Shapiro-Wilk normality test (GraphPad Prism v.8 software) and considered normal where values were over significance cut off ($P > 0.05$). Variance homogeneity was analysed using the F-test. All data are expressed as means \pm Standard Deviation (SD). $P < 0.05$ was considered statistically significant and $P < 0.1$ was considered as a non-significant trend towards significance.

Results

Advanced maternal age (AMA) delays embryo development at E3.5

At E3.5, embryos were collected from Young (7-8 weeks) and Old (7-8 months) C57/BL6 mothers and developmental stage assessed (Table 1). Whilst no difference was observed between Young and Old mice in dams becoming pregnant, embryo development was delayed in Old mothers with fewer blastocysts formed ($P < 0.05$), more present at an earlier stage of expansion ($P < 0.05$), and at non-significant trend for more morulae and arrested/degenerate embryos ($P < 0.1$) compared with Young mothers (Table 1) (Figure 1).

AMA did not affect derivation efficiency of mESC lines

Mouse ESC lines were derived from E3.5 blastocysts of Young and Old dams and cultured on MMC-MEFs in mESC medium. ICM outgrowths were cultured individually and each mESC line was generated from an individual blastocyst. No differences were found in the derivation efficiency of mESC lines isolated from individual Old dams (45%) compared to Young dams (36%). The number of male mESC lines (86 % in Old; 90% in Young) isolated was higher than female lines for both groups, hence effects of maternal age were evaluated only between male mESC lines. However, sex comparisons were made within the Old group.

mESC lines from Old mothers show chromosomal abnormalities

For karyotype analysis, 70% confluent mESC lines (P10-11) were treated with colcemid and hypotonic solution (KCl), and slides stained with Giemsa. From each mESC line, at least 70 chromosome spreads were counted and categorised as euploid ($2x = 40$), aneuploid ($2x \neq 40$), or polyploid ($2x \geq 80$) and only those lines with more than 50% euploidy were selected for further experiments. Since mESC karyotype may vary with extended in vitro culture²⁸ and

lines with apparent normal karyotype (>50%) may have a specific aneuploidy with a higher number of spreads with 38, 39 or 41 chromosomes²⁹, aneuploid spreads were further grouped into $2x \leq 37$, $2x = 38$ and $2x = 39$ (Table 2). Old male mESCs showed reduced euploidy and consequently increased total aneuploidy ($2x \neq 40$, $P = 0.024$) than Young male lines (Table 2). Old male mESCs had increased number of spreads with less than 37 chromosomes ($2x < 37$, $P = 0.008$), with 37 ($2x = 37$, $P = 0.033$) and, at non-significant trend, with 38 ($2x = 38$, $P = 0.090$) chromosomes, compared to Young male mESC lines. No differences were found between polyploidy levels ($2x \geq 80$). Separated by sex, Old male lines showed greater number of cells with 38 chromosomes ($2x = 38$, $P = 0.03$) compared to Old female lines, although no differences were observed between euploidy (Table 2).

Effect of AMA on pluripotency and differentiation marker expression of derived mESCs

Pluripotency of stem cells is typically divided into naïve and primed states³⁰. Collectively, AMA did not affect the relative mRNA expression of the naïve pluripotency markers *Oct4*, *Nanog* and *Lif* but Old male mESCs showed reduced *Sox2* expression ($P=0.049$) compared to Young male lines (Figure 2A). Flow cytometry assisted intracellular (nuclear) staining revealed no significant effect of AMA on the pluripotent protein expression (i.e. OCT4, NANOG, and SOX2) of the Old male and Young male mESC lines after 4 days culture (Figure 2B). However, OCT4 expression appears dynamically regulated over 0-96 h culture with a higher proportion of Young male cells expressing OCT4 up to 48 h ($P < 0.001$) compared with Old male lines, and while both lines diminish OCT4 expression at 72 h, this is slower in Old male lines ($P < 0.05$; Figure 2C). Sexually dimorphic differences were observed within the Old group, where the Old

Female mESC lines displayed reduced NANOG-expressing mESCs (P=0.033) compared to the Old Male group (Figure 2B).

Maternal age did not influence the gene expression of mesodermal (*Brachyury*) or endodermal (*Gata4*) transcripts in cell lines maintained in undifferentiated state (Figure 2A). However, Old male mESC lines had, a non-significant trend for reduced transcript levels of *Fgf10* (P=0.0573), important in cardiomyocyte differentiation, and *Tgf- α* (P=0.0522), important in regulating cell proliferation and apoptosis (Figure 2A) but no differences in other signalling and proliferation markers (*mTOR*, *Gsk3b*, *Akt1*, *Mapk1*). No sex-induced differences were observed within the Old mESC group for these markers (Figure 2A).

For qualitative analysis, mESC lines were cultured at the same starting density for 4 days (as used in FACS) before immunocytochemistry for OCT4, SOX2, BRACHYURY and Dapi nuclear staining (Figure 2D-F). Strong expression of OCT4 and SOX2 was present in both Young and Old male lines (Figure 2D, E). Old Female mESC lines however, showed relatively weak staining and smaller colonies compared to Old Male lines. Old Male and Female lines displayed similar staining for BRACHYURY which was not detected in Young male mESC lines (Figure 2F).

Effect of AMA on cell proliferation and viability of derived mESCs

Cell lines were seeded (27,000 cells/well) on 24-well plates for 96 h and harvested every 24 h. Phase contrast images indicated Young male lines (Figure 3A) to have more and larger colonies

at all time points compared to Old male mESC lines (Figure 3B), whereas Old Female mESC lines (Figure 3C) had the smallest and least number of colonies at all time points. For analysis, mESCs were separated into unattached (dead) and adherent cells at each time point; adherent cells were trypsinized and stained with viability dye, trypan blue (TB) to distinguish live (TB negative) and dead (TB positive) cells. Young male mESC lines had a higher proportion (P=0.001) and increased number (P<0.001) of live adherent cells compared to Old male mESC lines at all time points (Figure 3D). Consequently, Young male lines had fewer unattached (dead) cells (P<0.001) compared to Old male lines at 48 h (P= 0.0004) and 72 h (P= 0.015) (Figure 3E). Relative to Old males, Old female lines had an increased proportion of live cells at 48 h (P= 0.0493) with a consequent decrease in unattached/dead cells (Figure 3D, E). All groups showed increased rate of cell growth (P<0.001) over the first 3 days of culture, before reducing by day 4, as expected. (Figure 3D).

Proliferation was further assessed over 24-96 h culture by the level of nuclear-specific biomarker of cellular growth, Ki67³¹ in viable cells using FACS (Figure 3F). In agreement with the direct proliferation analysis, Ki67 expression was increased in Young male mESC lines compared to Old male mESC lines at 24 h (P = 0.01) and 48 h (P = 0.001; Figure 3F) while sex-associated differences were not observed within the Old mESC lines.

Cell apoptosis and death analysis of derived AMA mESCs

We assessed whether the reduced proportion of live cells and proliferation in Old male mESC lines was contributed to by increased apoptosis or cell death assessed by protein expression of

Annexin V- FITC and PI using FACS. Cell lines were seeded at defined cell density and analysed every 24 h for up to 96 h. Cells were selected from combined mESCs and MEFs using the pluripotency surface marker, Stage-Specific Embryonic Antigen-1 (SSEA-1) which did not differ between Young and Old male lines (data not shown). SSEA-1 positive cells were further separated into Annexin V and PI negative (live cells), Annexin V positive and PI negative (early apoptotic cells), Annexin V and PI positive (late apoptotic or necrotic cells), and Annexin V negative and PI positive (dead cells). Data are presented as proportion positive of total cells (stained and unstained cells) (Figure 4). Young and Old male lines had similar proportions of live cells at each time point (Figure 4A) and also of early apoptotic cells (Figure 4B). However, differences between Old male and female lines were found including a non-significant trend for more early apoptotic cells in female lines at 24 h but fewer at later time points ($P < 0.1$; Figure 4B). Old male lines had a non-significant trend for increased late apoptotic or necrotic cells when compared to Young male lines at 24 and 48 h ($P < 0.1$) and these cells were increased in Old female lines compared to male lines ($P < 0.05$; Figure 4C). Old female lines were also increased in dead cells at 48 h compared to Old male cells (Annexin negative / PI positive; $P < 0.01$) but no differences were detected between Young and Old male lines (Figure 4D). Overall, Old Female lines had a non-significant trend for decreased live ($P = 0.095$) and significantly increased necrotic ($P = 0.003$) proportion of total cells compared to Old Male lines (Figure 4A, C).

We next assessed mRNA expression of cyclin dependent kinase inhibitors *p19* and *p21* and cysteine dependent proteases in apoptosis of initiator (*caspase 9*), executor (*caspase 3*) and

inflammatory (*caspase 1*) caspases (Figure 4E). Although no age- or sex-induced differences were observed, Old male mESCs showed a non-significant increase in mean transcript levels for all markers compared to Young male lines.

Effect of AMA on expression of epigenetic modifiers and glucose transportation

The effect of AMA on mRNA expression of epigenetic modifiers including DNA methyl transferases (*Dnmt1*, *Dnmt3L*, *Dnmt3a*, *Dnmt3b*) and histone deacetylases (*Hdac-1*, *Hdac-3*) was assessed. Old male lines showed reduced *Dnmt3a* expression ($P = 0.049$) compared to Young male lines (Figure 5A). Old male lines also had a non-significant trend for reduced expression of *Dnmt3b* compared to Old female lines ($P < 0.1$; Figure 5A). No age or sex related differences were observed for *Hdac1* or *Hdac3*.

We further analysed expression of metabolic regulators across cell lines including mRNA expression of glucose and insulin metabolizers *Gapdh*, *InsR*, *Igf1* and *Igf1R*, and glucose transporter isoforms *Glut1*, *Glut3*, *Glut4* and *Glut8* (Figure 5B). Here, Old male mESC lines had a non-significant trend for reduced glucose transporter *Glut4* levels ($P = 0.0685$; Figure 5B) while Old female lines had reduced levels of the glycolytic enzyme *Gapdh* ($P = 0.029$) and a non-significant trend for reduced glucose transporter, *Glut8* ($P = 0.055$) compared with Old male lines (Figure 5B).

Discussion

We have investigated the effects of advanced maternal age (AMA) on mouse blastocyst development and the phenotype of undifferentiated mESCs derived from the ICM. Our primary objective was to develop a model for molecular and cellular analysis of early mechanisms contributing to the poorer fertility and health outcomes known to occur, independent of maternal somatic senescence, as a consequence of AMA^{1,6,7,14,15}. Our model of AMA used 7-8 month females when the decline in fertility is manifest by reduced oestrus cycles, decreased breeding performance with litter size and number of live births declining^{32,33} and so is broadly comparable to ~40 year old human in terms of age-related reproductive senescence. However, whilst we recognise across different bodily systems, comparison of mouse and human senescence may be complex, with ‘middle age’ compared as 10-14 months versus 37-48 years, respectively³⁴, the current focus was on reproductive potential to ensure our model had clinical relevance.

From our previous studies on the effects of maternal undernutrition on early embryo developmental potential, we have shown that derived mESCs do indeed exhibit and retain molecular and cellular changes in phenotype after several passages that match the *in vivo* condition and facilitate understanding of early mechanisms of adverse programming of health^{35,36}. This has also been shown in one study for mESCs derived from ART treatments to assess phenotypic changes¹⁹ but in another, mESC stability did not retain ART-mediated effects which may reflect strain differences³⁷. This strategy can therefore help overcome the inaccessibility and limited size of the pre- and peri-implantation embryo *in vivo* and reduce animal use in biomedical research.

Our data revealed AMA induced delay in embryo development (E3.5) but did not affect the derivation efficiency of mESC lines nor the strong bias of male over female cell lines. Female ESC lines are more prone to developing abnormal karyotypes related to reduced cellular function and proliferation^{24,38}. Collectively, mESCs from male AMA blastocysts exhibited a higher incidence of aneuploidy and karyotypic abnormalities, particularly increased occurrence of < 40 chromosomes. Normal karyotype AMA lines also displayed an altered pattern of expression of pluripotency genes and evidence of increased cellular senescence with poorer proliferation and increased incidence of late apoptotic cells. Lastly, AMA mESC lines exhibited reduced expression of genes important in critical cellular processes including epigenetic, metabolic and differentiation pathways. AMA lines also exhibited differences in these criteria dependent upon sex. Thus, these new cell lines exhibit all the characteristics expected of undifferentiated mESCs, but since they have not yet been used to generate chimeras with full development of all three germ layers, in strict terms, they are mESC-like.

Whilst derivation and *in vitro* culture of mESC lines may potentially increase the risk of epigenetic abnormalities over time and increasing passage number^{39,40}, we consider this unlikely here since passages have been limited and culture of both Old and Young lines normalised throughout experiments. Thus, differences observed between the treatments would already be established and programmed before derivation, permitting the AMA lines to provide a model for analysis of cellular mechanisms of aging on developmental potential.

The reduced viability and retarded rate of blastocyst development found in the Old group mirrors that shown previously^{19,41}. Poorer AMA fertility can derive from a combination of maternal cellular deficiencies including reduced mitochondrial efficiency and energy production, increased oxidative stress and declining steroid hormone levels, all of which may contribute to chromosomal and spindle errors as well as reduced early embryo viability⁴²⁻⁴⁵. Indeed, microarray analysis of aged metaphase II mouse oocytes reveal significant altered expression of genes involved in chromatin and spindle organisation, mitochondrial function and oxidative stress^{46,47} with a similar pattern evident in the human⁴⁸, and some but not all pathways altered at the proteomic level⁴⁹. Moreover, pharmacological treatments to overcome such cellular deficiencies can reverse these effects of aging^{50,51}. In our previous study on AMA in this strain of mice, blastocysts from aged dams also showed fewer trophectoderm and total cells compared with controls¹⁵. Collectively, these oocyte-derived perturbations continue into post-implantation concepti with abnormalities in fetal and placental morphology⁵².

Whilst embryos from Old mothers showed characteristic poorer quality and viability, ESC derivation efficiency was similar to Young embryos. However, early passage mESCs showed increased incidence of aneuploidy typical of the AMA phenotype *in vivo*. In particular, Old male lines exhibited increased percentage of karyotype with 38 or less chromosomes than Young male lines but no differences in incidence of polyploidy, suggesting instability to be chromosome-specific, as has been shown for mESCs in general²⁹. The increase in aneuploidy provides authentication of the AMA phenotype known to contribute to the reduced fertility of

older women in ART⁵³. Indeed, excess aneuploidy is also found in an ART model of mESC formation and increased by maternal age¹⁹.

Alterations in pluripotency marker expression was one notable characteristic of AMA mESC lines. Whilst these lines had normal expression of the naïve pluripotency markers *Oct4*, *Nanog* and *Lif*, AMA lines showed reduced *Sox2* expression and an altered profile over time of OCT4 expression at the protein level, reduced in early cultures but sustained in later cultures. The reduction in *Sox2* expression may reduce overall pluripotency and increase differentiation of ESCs by disturbing the positive-feedback loop between core-regulatory transcription factors essential in maintaining pluripotency as well as continuous ESC self-renewal⁵⁴⁻⁵⁷. In so doing, the reduction in *Sox2* expression may contribute to the observed dynamic changes in OCT4 expression. Like other pluripotency factors, SOX2 not only maintains self-renewal but assists in proliferation of ES cells⁵⁸, so may also contribute to the reduced proliferation and cell survival found in the Old mESC lines.

Old male mESC lines showed an increased proportion of dead cells, reduced live cells, reduced cell proliferation by Ki67 FACS analysis, reduced expression of the mitogen *Tgfa*, and increased proportion of late apoptotic/necrotic cells by Annexin V- PI FACS assay. Although the cyclin dependent kinase inhibitors (*p19* and *p21*) and apoptosis markers (*caspase 9*, *caspase 3* and *caspase 1*) showed no transcriptional differences between the groups, Old male mESCs showed increased mean transcript levels for all markers compared to Young male mESC lines. Collectively, these data warrant further evaluation of the role of altered pluripotency expression

in this outcome as well as cell death mechanisms such as the Ras/Raf/extracellular signal-regulated kinase (*Erk*) signalling pathway ⁵⁹.

The AMA male lines also showed differences in gene expression associated with other cellular processes compared to the control lines. *Dnmt3*, the key de novo DNA methylation regulator in development, is reduced in Old versus Young male lines which has implications for the epigenetic restructuring that occurs in the embryonic genome during post-implantation lineage allocation ⁶⁰. Consistent with this result, aged oocytes and embryos show reduced DNA methylation both *in vivo* and *in vitro* ⁶¹. In stem cells, de novo DNA methyltransferases maintain self-renewal, pluripotency and, therefore, affect proliferation and differentiation capacity of these cells ⁶² suggesting this epigenetic deficiency may contribute more broadly to our AMA mESC phenotype. Similarly, the reduction in expression of *Fgf10* in Old male lines may affect cardiomyocyte differentiation since it plays a critical role in cardiac development in the embryo ⁶³. Poor cardiac function and hypertension has been shown to be symptomatic of adult offspring in response to adverse periconceptional developmental programming from diverse environments including maternal undernutrition and ART treatments ¹⁶. Moreover, mouse maternal aging leads to increased blood pressure and reduced heart size in offspring ¹⁵.

Phenotypic differences were also observed in the AMA lines dependent upon sex. Female lines displayed reduced *Nanog* expression and showed relatively weak staining and smaller colonies compared to male lines. Female AMA lines also displayed increased incidence of apoptotic/necrotic cells than male lines and had differences in level of expression of epigenetic

and metabolic genes. Developmental programming has consistently shown differences in phenotype and outcomes between male and female offspring¹⁶ including in response to AMA¹⁵. Sex-dependent differences in susceptibility to disease usually arise in utero⁶⁴. Moreover, environmental factors are known to differentially influence cell signalling, gene expression and morphogenesis during development dependent upon sex that can be maintained into postnatal life⁶⁵.

In conclusion, we have shown that AMA leads to a retardation in preimplantation development and a complex series of phenotypic effects in derived mESC lines at chromosomal, molecular and cellular levels. These perturbations affect pluripotency, cell proliferation and apoptosis with potential to alter epigenetic and differentiative mechanisms throughout development. These novel cell lines derived from natural embryo development provide a model to investigate early mechanisms of AMA effect on developmental programming in the absence of confounding maternal senescence.

Acknowledgements

We thank the Biomedical Research Facility staff for animal technical support and the Faculty Flow Cytometry Unit staff for FACS support.

Financial support

This work was supported through the European Union FP7-PEOPLE-2012-ITN EpiHealthNet programme (317146) and FP7-CP-FP Epihealth programme (278418) to T.P.F. and the BBSRC (BB/F007450/1) to T.P.F.

Author contribution

PK performed experiments, analysed data, drafted and edited the manuscript.

NRS provided technical and training support, analysed data and edited the paper.

BS provided technical and training support.

MAV provided technical and training support, edited the manuscript.

JJE provided technical and training support and edited the manuscript

TPF conceived and designed the study, drafted and edited the manuscript.

References

1. Crawford NM, Steiner AZ. Age-related infertility. *Obstetrics and gynecology clinics of North America* 2015; **42**(1): 15-25.
2. Biro MA, Davey MA, Carolan M, Kealy M. Advanced maternal age and obstetric morbidity for women giving birth in Victoria, Australia: A population-based study. *Aust N Z J Obstet Gynaecol* 2012; **52**(3): 229-34.
3. Delbaere I, Verstraelen H, Goetgeluk S, Martens G, De Backer G, Temmerman M. Pregnancy outcome in primiparae of advanced maternal age. *European journal of obstetrics, gynecology, and reproductive biology* 2007; **135**(1): 41-6.

- 541 4. Carolan M. Maternal age ≥ 45 years and maternal and perinatal outcomes: a review of the
542 evidence. *Midwifery* 2013; **29**(5): 479-89.
- 543 5. Ferré C, Callaghan W, Olson C, Sharma A, Barfield W. Effects of Maternal Age and Age-Specific
544 Preterm Birth Rates on Overall Preterm Birth Rates - United States, 2007 and 2014. *MMWR Morb Mortal*
545 *Wkly Rep* 2016; **65**(43): 1181-4.
- 546 6. Tearne JE, Robinson M, Jacoby P, et al. Older maternal age is associated with depression,
547 anxiety, and stress symptoms in young adult female offspring. *J Abnorm Psychol* 2016; **125**(1): 1-10.
- 548 7. Cooke CM, Davidge ST. Advanced maternal age and the impact on maternal and offspring
549 cardiovascular health. *American journal of physiology Heart and circulatory physiology* 2019; **317**(2):
550 H387-h94.
- 551 8. Nagaoka SI, Hassold TJ, Hunt PA. Human aneuploidy: mechanisms and new insights into an age-
552 old problem. *Nat Rev Genet* 2012; **13**(7): 493-504.
- 553 9. Jones KT, Lane SI. Molecular causes of aneuploidy in mammalian eggs. *Development* 2013;
554 **140**(18): 3719-30.
- 555 10. Nakagawa S, FitzHarris G. Intrinsically Defective Microtubule Dynamics Contribute to Age-
556 Related Chromosome Segregation Errors in Mouse Oocyte Meiosis-I. *Current biology : CB* 2017; **27**(7):
557 1040-7.
- 558 11. Cano F, Simón C, Remohí J, Pellicer A. Effect of aging on the female reproductive system:
559 evidence for a role of uterine senescence in the decline in female fecundity. *Fertil Steril* 1995; **64**(3): 584-
560 9.
- 561 12. Woods L, Perez-Garcia V, Kieckbusch J, et al. Decidualisation and placentation defects are a
562 major cause of age-related reproductive decline. *Nature communications* 2017; **8**(1): 352.
- 563 13. Shirasuna K, Iwata H. Effect of aging on the female reproductive function. *Contracept Reprod*
564 *Med* 2017; **2**: 23.
- 565 14. Janny L, Menezo YJ. Maternal age effect on early human embryonic development and blastocyst
566 formation. *Mol Reprod Dev* 1996; **45**(1): 31-7.
- 567 15. Velazquez MA, Smith CG, Smyth NR, Osmond C, Fleming TP. Advanced maternal age causes
568 adverse programming of mouse blastocysts leading to altered growth and impaired cardiometabolic
569 health in post-natal life. *Hum Reprod* 2016; **31**(9): 1970-80.
- 570 16. Fleming TP, Watkins AJ, Velazquez MA, et al. Origins of lifetime health around the time of
571 conception: causes and consequences. *Lancet* 2018; **391**(10132): 1842-52.
- 572 17. McCallie BR, Parks JC, Trahan GD, et al. Compromised global embryonic transcriptome
573 associated with advanced maternal age. *Journal of assisted reproduction and genetics* 2019; **36**(5): 915-
574 24.

- 575 18. Huang J, Okuka M, Wang F, et al. Generation of pluripotent stem cells from eggs of aging mice.
576 *Aging Cell* 2010; **9**(2): 113-25.
- 577 19. Assadollahi V, Fathi F, Abdi M, Khadem Erfan MB, Soleimani F, Banafshi O. Increasing maternal
578 age of blastocyst affects on efficient derivation and behavior of mouse embryonic stem cells. *J Cell*
579 *Biochem* 2019; **120**(3): 3716-26.
- 580 20. Yagi T, Tokunaga T, Furuta Y, et al. A novel ES cell line, TT2, with high germline-differentiating
581 potency. *Anal Biochem* 1993; **214**(1): 70-6.
- 582 21. Nasr-Esfahani M, Johnson MH, Aitken RJ. The effect of iron and iron chelators on the in-vitro
583 block to development of the mouse preimplantation embryo: BAT6 a new medium for improved culture
584 of mouse embryos in vitro. *Hum Reprod* 1990; **5**(8): 997-1003.
- 585 22. Summers MC, McGinnis LK, Lawitts JA, Raffin M, Biggers JD. IVF of mouse ova in a simplex
586 optimized medium supplemented with amino acids. *Hum Reprod* 2000; **15**(8): 1791-801.
- 587 23. Ramírez-Solis R, Rivera-Pérez J, Wallace JD, Wims M, Zheng H, Bradley A. Genomic DNA
588 microextraction: a method to screen numerous samples. *Anal Biochem* 1992; **201**(2): 331-5.
- 589 24. Zvetkova I, Apedaile A, Ramsahoye B, et al. Global hypomethylation of the genome in XX
590 embryonic stem cells. *Nat Genet* 2005; **37**(11): 1274-9.
- 591 25. Campos PB, Sartore RC, Abdalla SN, Rehen SK. Chromosomal spread preparation of human
592 embryonic stem cells for karyotyping. *Journal of visualized experiments : JoVE* 2009; (31).
- 593 26. Radonić A, Thulke S, Mackay IM, Landt O, Siegert W, Nitsche A. Guideline to reference gene
594 selection for quantitative real-time PCR. *Biochemical and biophysical research communications* 2004;
595 **313**(4): 856-62.
- 596 27. Vandesompele J, De Preter K, Pattyn F, et al. Accurate normalization of real-time quantitative
597 RT-PCR data by geometric averaging of multiple internal control genes. *Genome biology* 2002; **3**(7):
598 Research0034.
- 599 28. Rebuzzini P, Zuccotti M, Redi CA, Garagna S. Chromosomal Abnormalities in Embryonic and
600 Somatic Stem Cells. *Cytogenet Genome Res* 2015; **147**(1): 1-9.
- 601 29. Gaztelumendi N, Nogués C. Chromosome instability in mouse embryonic stem cells. *Scientific*
602 *reports* 2014; **4**: 5324.
- 603 30. Davidson KC, Mason EA, Pera MF. The pluripotent state in mouse and human. *Development*
604 2015; **142**(18): 3090-9.
- 605 31. Preusser M, Heinzl H, Gelpi E, et al. Ki67 index in intracranial ependymoma: a promising
606 histopathological candidate biomarker. *Histopathology* 2008; **53**(1): 39-47.
- 607 32. Nelson JF, Felicio LS, Randall PK, Sims C, Finch CE. A longitudinal study of estrous cyclicity in
608 aging C57BL/6J mice: I. Cycle frequency, length and vaginal cytology. *Biol Reprod* 1982; **27**(2): 327-39.

609 33. Guo R, Pankhurst MW. Accelerated ovarian reserve depletion in female anti-Müllerian hormone
610 knockout mice has no effect on lifetime fertility†. *Biol Reprod* 2020; **102**(4): 915-22.

611 34. Flurkey K CJ, Harrison DE. The mouse in aging research. . In: Fox JG BS, Davisson MT, Newcomer
612 CE, Quimby FW, Smith AL, ed. The Mouse in Biomedical Research. 2nd ed. Burlington, MA: Elsevier
613 Academic Press; 2007: 637-72.

614 35. Sun C, Velazquez MA, Marfy-Smith S, et al. Mouse early extra-embryonic lineages activate
615 compensatory endocytosis in response to poor maternal nutrition. *Development* 2014; **141**(5): 1140-50.

616 36. Sun C, Denisenko O, Sheth B, et al. Epigenetic regulation of histone modifications and Gata6
617 gene expression induced by maternal diet in mouse embryoid bodies in a model of developmental
618 programming. *BMC developmental biology* 2015; **15**(1): 3.

619 37. Simbulan RK, Di Santo M, Liu X, et al. Embryonic stem cells derived from in vivo or in vitro-
620 generated murine blastocysts display similar transcriptome and differentiation potential. *PLoS One*
621 2015; **10**(2): e0117422.

622 38. Hadjantonakis A, Papaioannou V. The stem cells of early embryos. *Differentiation* 2001; **68**(4-5):
623 159-66.

624 39. Huntriss J, Picton HM. Stability of genomic imprinting in embryonic stem cells: lessons from
625 assisted reproductive technology. *Curr Stem Cell Res Ther* 2008; **3**(2): 107-16.

626 40. Horii T, Yanagisawa E, Kimura M, Morita S, Hatada I. Epigenetic differences between embryonic
627 stem cells generated from blastocysts developed in vitro and in vivo. *Cell Reprogram* 2010; **12**(5): 551-
628 63.

629 41. Fu X, Cheng J, Hou Y, Zhu S. The association between the oocyte pool and aneuploidy: a
630 comparative study of the reproductive potential of young and aged mice. *Journal of assisted*
631 *reproduction and genetics* 2014; **31**(3): 323-31.

632 42. Davison SL, Bell R, Donath S, Montalto JG, Davis SR. Androgen levels in adult females: changes
633 with age, menopause, and oophorectomy. *J Clin Endocrinol Metab* 2005; **90**(7): 3847-53.

634 43. Ben-Meir A, Burstein E, Borrego-Alvarez A, et al. Coenzyme Q10 restores oocyte mitochondrial
635 function and fertility during reproductive aging. *Aging Cell* 2015; **14**(5): 887-95.

636 44. Meldrum DR, Casper RF, Diez-Juan A, Simon C, Domar AD, Frydman R. Aging and the
637 environment affect gamete and embryo potential: can we intervene? *Fertil Steril* 2016; **105**(3): 548-59.

638 45. May-Panloup P, Brochard V, Hamel JF, et al. Maternal ageing impairs mitochondrial DNA kinetics
639 during early embryogenesis in mice. *Hum Reprod* 2019; **34**(7): 1313-24.

640 46. Hamatani T, Falco G, Carter MG, et al. Age-associated alteration of gene expression patterns in
641 mouse oocytes. *Human molecular genetics* 2004; **13**(19): 2263-78.

642 47. Pan H, Ma P, Zhu W, Schultz RM. Age-associated increase in aneuploidy and changes in gene
643 expression in mouse eggs. *Dev Biol* 2008; **316**(2): 397-407.

644 48. Grøndahl ML, Yding Andersen C, Bogstad J, Nielsen FC, Meinertz H, Borup R. Gene expression
645 profiles of single human mature oocytes in relation to age. *Hum Reprod* 2010; **25**(4): 957-68.

646 49. Schwarzer C, Siatkowski M, Pfeiffer MJ, et al. Maternal age effect on mouse oocytes: new
647 biological insight from proteomic analysis. *Reproduction* 2014; **148**(1): 55-72.

648 50. Silva E, Greene AF, Strauss K, Herrick JR, Schoolcraft WB, Krisher RL. Antioxidant
649 supplementation during in vitro culture improves mitochondrial function and development of embryos
650 from aged female mice. *Reprod Fertil Dev* 2015; **27**(6): 975-83.

651 51. Yoon J, Juhn KM, Jung EH, et al. Effects of resveratrol, granulocyte-macrophage colony-
652 stimulating factor or dichloroacetic acid in the culture media on embryonic development and pregnancy
653 rates in aged mice. *Aging (Albany NY)* 2020; **12**(3): 2659-69.

654 52. Lopes FL, Fortier AL, Darricarrère N, Chan D, Arnold DR, Trasler JM. Reproductive and epigenetic
655 outcomes associated with aging mouse oocytes. *Human molecular genetics* 2009; **18**(11): 2032-44.

656 53. Harton GL, Munné S, Surrey M, et al. Diminished effect of maternal age on implantation after
657 preimplantation genetic diagnosis with array comparative genomic hybridization. *Fertil Steril* 2013;
658 **100**(6): 1695-703.

659 54. Ivanova N, Dobrin R, Lu R, et al. Dissecting self-renewal in stem cells with RNA interference.
660 *Nature* 2006; **442**(7102): 533-8.

661 55. Boer B, Kopp J, Mallanna S, et al. Elevating the levels of Sox2 in embryonal carcinoma cells and
662 embryonic stem cells inhibits the expression of Sox2:Oct-3/4 target genes. *Nucleic acids research* 2007;
663 **35**(6): 1773-86.

664 56. Masui S, Nakatake Y, Toyooka Y, et al. Pluripotency governed by Sox2 via regulation of Oct3/4
665 expression in mouse embryonic stem cells. *Nature cell biology* 2007; **9**(6): 625-35.

666 57. Kopp JL, Ormsbee BD, Desler M, Rizzino A. Small increases in the level of Sox2 trigger the
667 differentiation of mouse embryonic stem cells. *Stem Cells* 2008; **26**(4): 903-11.

668 58. Thomson M, Liu SJ, Zou LN, Smith Z, Meissner A, Ramanathan S. Pluripotency factors in
669 embryonic stem cells regulate differentiation into germ layers. *Cell* 2011; **145**(6): 875-89.

670 59. Cagnol S, Chambard JC. ERK and cell death: mechanisms of ERK-induced cell death--apoptosis,
671 autophagy and senescence. *Febs j* 2010; **277**(1): 2-21.

672 60. Smallwood SA, Kelsey G. De novo DNA methylation: a germ cell perspective. *Trends Genet* 2012;
673 **28**(1): 33-42.

674 61. Yue MX, Fu XW, Zhou GB, et al. Abnormal DNA methylation in oocytes could be associated with
675 a decrease in reproductive potential in old mice. *Journal of assisted reproduction and genetics* 2012;
676 **29**(7): 643-50.

62. Tadokoro Y, Ema H, Okano M, Li E, Nakauchi H. De novo DNA methyltransferase is essential for self-renewal, but not for differentiation, in hematopoietic stem cells. *The Journal of experimental medicine* 2007; **204**(4): 715-22.

63. Hubert F, Payan SM, Rochais F. FGF10 Signaling in Heart Development, Homeostasis, Disease and Repair. *Frontiers in genetics* 2018; **9**: 599.

64. Schalekamp-Timmermans S, Cornette J, Hofman A, et al. In utero origin of sex-related differences in future cardiovascular disease. *Biol Sex Differ* 2016; **7**: 55.

65. Hansen PJ, Dobbs KB, Denicol AC, Siqueira LGB. Sex and the preimplantation embryo: implications of sexual dimorphism in the preimplantation period for maternal programming of embryonic development. *Cell and tissue research* 2016; **363**(1): 237-47.

Figure legends

Figure 1. Representative images of embryos derived from (A) Young (7-8 weeks) and (B) Old (7-8 months) female mice (C57BL/6 females mated with CBA males) at E3.5. Magnification bar = 200 μ m.

Figure 2. Pluripotent, differentiation and cell proliferation markers in undifferentiated Young (7-8 weeks) vs Old (7-8 months) male, and Old Male vs Old Female (7-8 months) mESC lines. (A) Genes of interest were normalized to *Ywhaz* and *Rpl13a* within geNorm; Old male mESC lines had reduced expression (qPCR) of *Sox2* ($P=0.049$), and non-significant trend reduction in *Fgf 10* ($P=0.0573$) and *Tgf α* ($P=0.0522$) relative to Young male lines. **(B)** Quantitative analysis of protein expression for pluripotent markers. No differences were identified between Old Male vs Young Male lines but Old Female mESCs had reduced NANOG expression ($P<0.05$); mESCs were cultured in triplicate with $n=4$ mESC lines per group. **(C)** Protein expression of OCT4 over time is distinct between Old and Young Male mESCs with

reduced expression at earlier times ($P < 0.001$) and sustained expression at later times ($P < 0.05$) in Old Male lines. **(D-E)** Qualitative immunocytochemistry images showed similar expression of pluripotent markers OCT4 and SOX2, and colony size in Young and Old Male mESC lines. Old Female lines however, showed reduced colony size with less relative expression of the pluripotent markers compared to the Old Male group. **(G)** Immunocytochemistry showed no expression of the mesodermal marker, BRACHYURY, in Young male lines although colonies stained positive in Old Male and Old Female lines. Magnification bar = 200 μm . Data presented as means \pm SDs based on $n = 4$ mESC lines per group examined in triplicate; $**P < 0.001$, $*P < 0.05$, $\Delta P < 0.1$ non-significant trend. Note: for **(A-C)**, comparisons between Old Male and Young Male for ageing effects and between Old Male and Old Female for sex effects were normalised and analysed by t-test separately hence without post-hoc correction and placed in same chart for conciseness.

Figure 3. Cell proliferation and viability of undifferentiated Young male (7-8 weeks), Old (7-8 months) male, and female mESC lines. **(A-C)** Representative phase-contrast images of cell proliferation of Young male, Old male and Old female mESCs. After seeding, images were captured every 24 h over a period of 96 h. Images show that Young male **(A)** mESC lines have larger colonies with increased density of cells/ colony compared to Old male **(B)** mESC lines. Old Female mESC lines **(C)** present much smaller colony size and fewer mESC clones compared to Old Male mESC lines. Arrows and parenthesis point toward the colony size differences across the groups. Magnification = 100 μm . **(D, E)** Trypan negative (live) cells are presented as proportion of adherent (live and dead) cells, and floating cells as proportion of total (live, dead

and floating) cells. **(D)** Old male mESC lines had fewer live adherent cells at all time points, and **(E)** increased proportion of floating cells at 48 h and 72 h, as compared to Young male mESC lines. **(F)** Protein expression of cell proliferation marker Ki67 over time presented as the proportion positive of total cells (stained and unstained). Ki67 expression was lower in Old vs Young mESC lines at 24 h ($P=0.011$) and 48 h ($P=0.001$). Data presented as means \pm SDs based on $n = 4$ mESC lines per group. * $P<0.01$, ** $P<0.001$, *** $P<0.0001$, **** $P<0.00001$. Note: for **(D-F)**, comparisons between Old Male and Young Male for ageing effects and between Old Male and Old Female for sex effects were normalised and analysed by t-test separately hence without post-hoc correction and placed in same chart for conciseness.

Figure 4. FACS analysis for detection of early apoptosis (Annexin V) and cell death (PI) in undifferentiated Young (7-8 weeks) vs Old (7-8 months) male, and Old male vs Old female (7-8 months) mESC lines. mESCs were cultured in duplicate. (A-D) Data is presented as proportion of total cells. Compared to the Young group, Old mESCs presented (C) increased necrosis at non-significant trend at 24 h ($P=0.075$) although the (B) proportion of early apoptotic cells was unaffected by age and time. Sex differences were observed within the Old mESC group where Old Female mESC lines showed (B) increased proportion of early apoptotic cells at non-significant trend ($P=0.059$) at 24 h, which decreased at 48 h ($P=0.055$) and 96 h ($P=0.085$) also at non-significant trend. Old Female mESC lines also exhibited increased proportion of (C) necrotic cells at 72 h ($P=0.035$) and 96 h ($P=0.035$), and (D) dead cells at 48 h ($P=0.01$) compared to Old male mESC lines. (E) However, RT-qPCR analysis of cell apoptotic markers

was unaffected by maternal age and sex. Data presented as means \pm SDs based on n = 4 mESC lines per group, where Δ = trending $P < 0.1$, * = $P < 0.05$ and ** = $P < 0.01$. Note: for (A-E), comparisons between Old Male and Young Male for ageing effects and between Old Male and Old Female for sex effects were normalised and analysed by t-test separately hence without post-hoc correction and placed in same chart for conciseness.

Figure 5. Relative gene expression for epigenetic modifiers and glucose transporters in undifferentiated Young (7-8 weeks) vs Old (7-8 months) male and Old male vs Old female (7-8 months) mESC lines. Real-time PCR analysis of DNA methyltransferases *Dnmt1*, *Dnmt3L*, *Dnmt3a* and *Dnmt3b*, histone modifiers *Hdac1* and *Hdac3*; glucose transporters *Glut1*, *Glut3*, *Glut4* and *Glut8* and metabolizers *Gapdh*, *InsR*, *Igf1* and *Igf1R*. Genes of interest were normalized to *Ywhaz* and *Rpl13a* within geNorm. (A, B) Old male mESC lines showed reduced expression of *Dnmt3a* ($P = 0.049$) and *Glut4* at non-significant trend level ($P = 0.0685$) compared to Young male mESC lines. Old Female mESC lines showed reduced expression of *Dnmt3b* at non-significant trend ($P = 0.078$) and increased relative expression of *Gapdh* ($P = 0.029$) and *Glut8* ($P = 0.055$) at non-significant trend compared to Old Male mESC lines. Data presented as means \pm SDs based on n = 4 mESC lines per group. * indicates $P < 0.05$ and Δ indicates trend $P < 0.1$. Note: for (A,B), comparisons between Old Male and Young Male for ageing effects and between Old Male and Old Female for sex effects were normalised and analysed by t-test separately hence without post-hoc correction and placed in same chart for conciseness.

Table 1. Embryo development from Young and Old female mice at E3.5.

Flushed at E3.5	Total number (%)	
	Young (7-8 weeks, n = 10)	Old (7-8 months, n = 10)
Arrested/Degenerate	9 (11.0)	18 (23.7)
Morulae	4 (4.9)	13 (17.2) †
Early blastocysts	6 (7.3)	14 (18.4) *
Mid blastocysts	52 (63.4)	20 (26.3) †
Late blastocysts	11 (13.4)	11 (14.5)
Total blastocysts	69 (84.1)	45 (59.2) *

Number (%) of embryos collected; n = number of dams. * P<0.05; † P<0.1

Table 2. Effect of maternal age on karyotype of mESCs lines derived from Young and Old dams.

Karyotype n	Chromosome spreads (%)		
	Young male 6	Old male 6	Old female 4
Euploidy ($2x = 40$)	67.4	41.65*	46.23
Total Aneuploidy ($2x \neq 40$)	32.6	58.35*	53.4
Segregation within Aneuploidy (%)			
$2x < 37$	8.35	18.41**	14.62
$2x = 37$	1.44	4.78*	6.08
$2x = 38$	3.02	5.67†	0.12*
$2x = 39$	5.5	8.58	8.24
$2x > 40, < 80$	9.24	20.35	12.13
$2x = 80$	3.27	1.43	0.72
$2x \geq 80$	1.78	0.25	0.24

Data presented as % chromosome spreads; n = number of cell lines analysed (70 spreads from each); x = number of chromosomes; ** $P < 0.01$; * $P < 0.05$, † $P < 0.1$ (Old males vs Young males; Old females vs Old males).

Supplementary Table S1. List of primer sequences used for q-PCR

Gene symbol	Forward sequence (5'- 3')	Reverse sequence (3'- 5')
<i>Akt1</i>	TCGTGTGGCAGGATGTGTAT	ACCTGGTGTCTAGTCTCAGAGG
<i>Brachyury</i>	GCTTCAAGGAGCTAACTAACGAG	CCAGCAAGAAAGAGTACATGGC
<i>Casp 1</i>	AGGCACGGGACCTATGTGAT	AGCTGATGGAGCTGATTGAAG
<i>Casp 8</i>	AGCACAGAGAGAAGAATGAGCC	TTGGCGAGTCACACAGTTCC
<i>Casp3</i>	GACTCCACTTTCCACGCAA	CCCACCCCCAATCATTCCT
<i>Dnmt 1</i>	GCTACCAGTGCACCTTTGGT	ATGATGGCCCTCCTTCGT
<i>Dnmt 3a</i>	ACACAGGGCCCGTTACTTCT	TCACAGTGGATGCCAAAGG
<i>Dnmt 3b</i>	GCCTGCAAGACTTCTTCACTACT	GGTACAACCTTGGGTGGCTCA
<i>Dnmt 3L</i>	AACCGACGGAGCATTGAA	CCGAGTGTACACCTGGAGACT
<i>EGF</i>	GGGCAGGAAACAAGTTCGT	CATGCCCCACAGGATTTG
<i>FGF-10</i>	AACAACCTCCGATTTCCACTGA	CGGGACCAAGAATGAAGACT
<i>FGF-4</i>	CGGAGAGAGCTCCAGAAGAC	TACCTGCTGGGCCTCAAA
<i>Gapdh</i>	Proprietary information (Primerdesign)	Proprietary information (Primerdesign)
<i>Gata4</i>	GGAAGACACCCCAATCTCG	CATGGCCCCACAATTGAC
<i>Glut 1</i>	ATGGATCCCAGCAGCAAG	CCAGTGTTATAGCCGAAGTGC
<i>Glut 3</i>	TTGCCCTGAGAGTCCAAGA	ACAAGCGCTGCAGGATCT
<i>Glut 8</i>	CCAGCGCCACTCTAGGAC	CAGCTGATGGTTGTCAGTGG
<i>Glut-4</i>	GTGGACTGGTTTCTGGACCG	CCTCAATCACCGAGTTCCCC
<i>Gsk3b</i>	GCACTCTTCAACTTTACCACTCAAG	CGAGCATGTGGAGGGATAAG
<i>Hdac1</i>	AATCCTGAACTGCCAAGTGC	AAGCCTGAAAAGGGGTCCTA
<i>Hdac3</i>	CTCTGGTGAAGGGTTTGGA	TGTCCATGTCTCATCCCTGA
<i>Igf-1</i>	GAAGACGACATGATGTGTATCTTTATC	AGCAGCCTTCCAACCTCAATTAT
<i>Igf1-R</i>	CACTTGCATGACGTCTCTCC	GAGAATTTCTTTCACAATTCCATC
<i>InsR</i>	TCTTTCTTCAGGAAGCTACATCTG	TGTCCAAGGCATAAAAAGAATAGTT
<i>LIF</i>	AGCAGCAGTAAGGGCACAAT	AAACGGCCTGCATCTAAGG
<i>MAPK-1</i>	CCTTCAGAGCACTCCAGAAAGT	ACAACACCAAAAAGGCATCC
<i>mTOR</i>	GTGGAAAAGTGCTCGGAAGA	CATGGTCTGCACAAAGTGTTG
<i>Nanog</i>	TGCTTACAAGGGTCTGCTACTG	GAGGCAGGTCTTCAGAGGAA
<i>Oct4</i>	GTTGGAGAAGGTGGAACCAA	CTCCTTCTGCAGGGCTTTC
<i>p19</i>	TGCTGGATTGCAGAGCAGTAA	GCATGCAGAGATTCCGAGAGA
<i>p21</i>	CCGAGAACGGTGGAACCTTTGAC	GAACGCGCTCCCAGACGAAGTTG
<i>Rpl13a</i>	Proprietary information (Primerdesign)	Proprietary information (Primerdesign)
<i>Sox2</i>	TGGGCTCTGTGGTCAAGTC	TGATCATGTCCCGGAGGT
<i>TGF-α</i>	ACGTACCCAGAGTGGCAGAC	GTGCCCAGATTCCCACAC
<i>Ywhaz</i>	Proprietary information (Primerdesign)	Proprietary information (Primerdesign)

Supplementary Table S2. List of antibodies used.**Flow cytometry**

Coupled antigen	Company	Catalog no.	Working dilution
NANOG-APC	Miltenyi Biotec	REA297	1:10
OCT3/4 Isoform A-APC	Miltenyi Biotec	REA622	1:10
SOX2-PE	Miltenyi Biotec	REA320	1:10
SSEA-1-APC	Miltenyi Biotec	REA321	1:10
Ki-67-FITC	Miltenyi Biotec	REA183	1:10
AnnexinV-FITC Kit	eBioscience	BMS500FI	Annexin-FITC 1:4 PI- 1:5

Immunocytochemistry

Antigen	Species	Company	Cat no.	Working Dilution
Nanog	Mouse	SantaCruz Biotechnology (SCBT)	293121	1:50
Oct4	Mouse	SCBT	5279	1:50
Sox2	Mouse	SCBT	365823	1:50
Gata4	Mouse	SCBT	25310	1:50
Brachyury	Mouse	SCBT	166962	1:50
Alexa 488	Goat	Abcam	A11008	1:1000
Alexa 594	Donkey	Abcam	A21203	1:1000

Figure 1

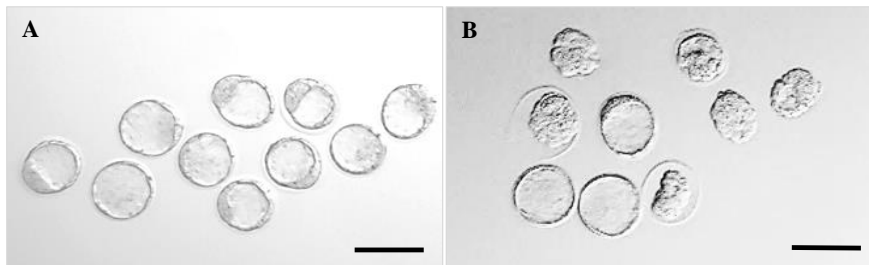
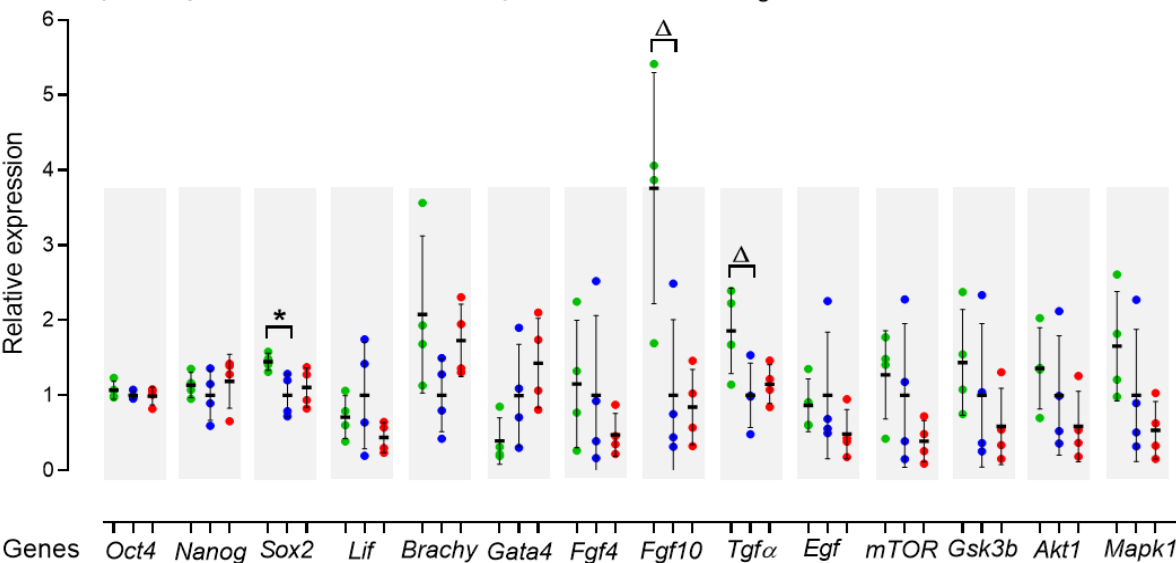


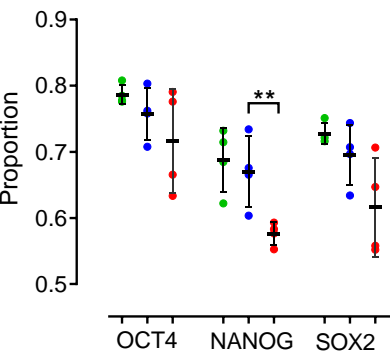
Figure 1 Representative images of embryos derived from (A) Young (7-8 weeks) and (B) Old (7-8 months) female mice (C57BL/6 females mated with CBA males) at E3.5. Magnification bar = 200 μm .

Figure 2

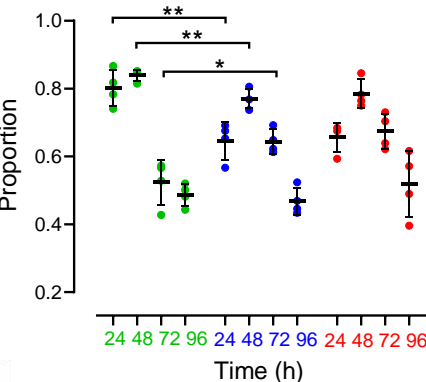
A. Pluripotency, differentiation and cell proliferation ● Young male ● Old male ● Old female



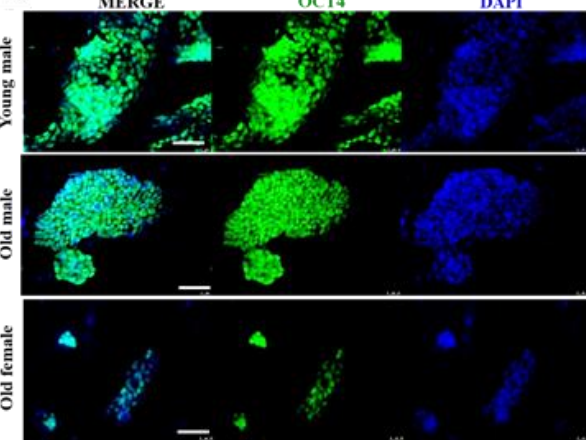
B. Pluripotency (protein expression)



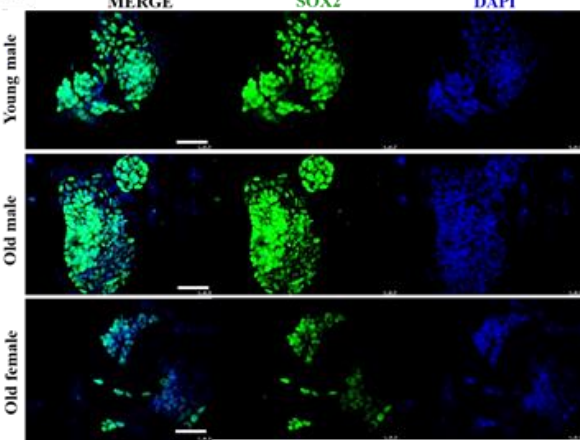
C. Oct 4



D



E



F

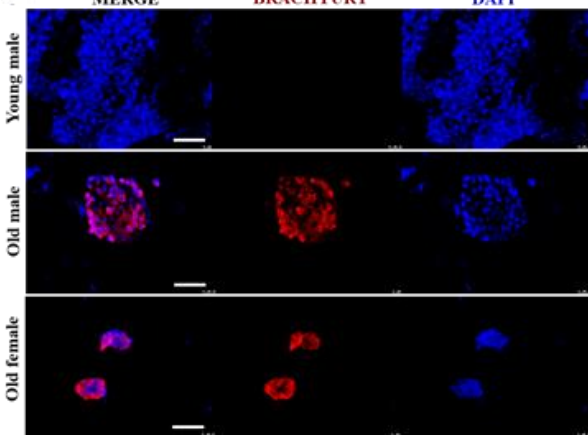


Figure 2. Pluripotent, differentiation and cell proliferation markers in undifferentiated Young (7-8 weeks) vs Old (7-8 months) male, and Old Male vs Old Female (7-8 months) mESC lines. (A) Genes of interest were normalized to *Ywhaz* and *Rpl13a* within geNorm; Old male mESC lines had reduced expression (qPCR) of *Sox2* ($P=0.049$), and non-significant trend reduction in *Fgf 10* ($P=0.0573$) and *Tgf α* ($P=0.0522$) relative to Young male lines. (B) Quantitative analysis of protein expression for pluripotent markers. No differences were identified between Old Male vs Young Male lines but Old Female mESCs had reduced NANOG expression ($P<0.05$); mESCs were cultured in triplicate with $n=4$ mESC lines per group. (C) Protein expression of OCT4 over time is distinct between Old and Young Male mESCs with reduced expression at earlier times ($P<0.001$) and sustained expression at later times ($P<0.05$) in Old Male lines. (D-E) Qualitative immunocytochemistry images showed similar expression of pluripotent markers OCT4 and SOX2, and colony size in Young and Old Male mESC lines. Old Female lines however, showed reduced colony size with less relative expression of the pluripotent markers compared to the Old Male group. (G) Immunocytochemistry showed no expression of the mesodermal marker, BRACHYURY, in Young male lines although colonies stained positive in Old Male and Old Female lines. Magnification bar = 200 μm . Data presented as means \pm SDs based on $n = 4$ mESC lines per group examined in triplicate; $**P<0.001$, $*P<0.05$, $\Delta P<0.1$ non-significant trend. Note: for (A-C), comparisons between Old Male and Young Male for ageing effects and between Old Male and Old Female for sex effects were normalised and analysed by t-test separately hence without post-hoc correction and placed in same chart for conciseness.

Figure 3

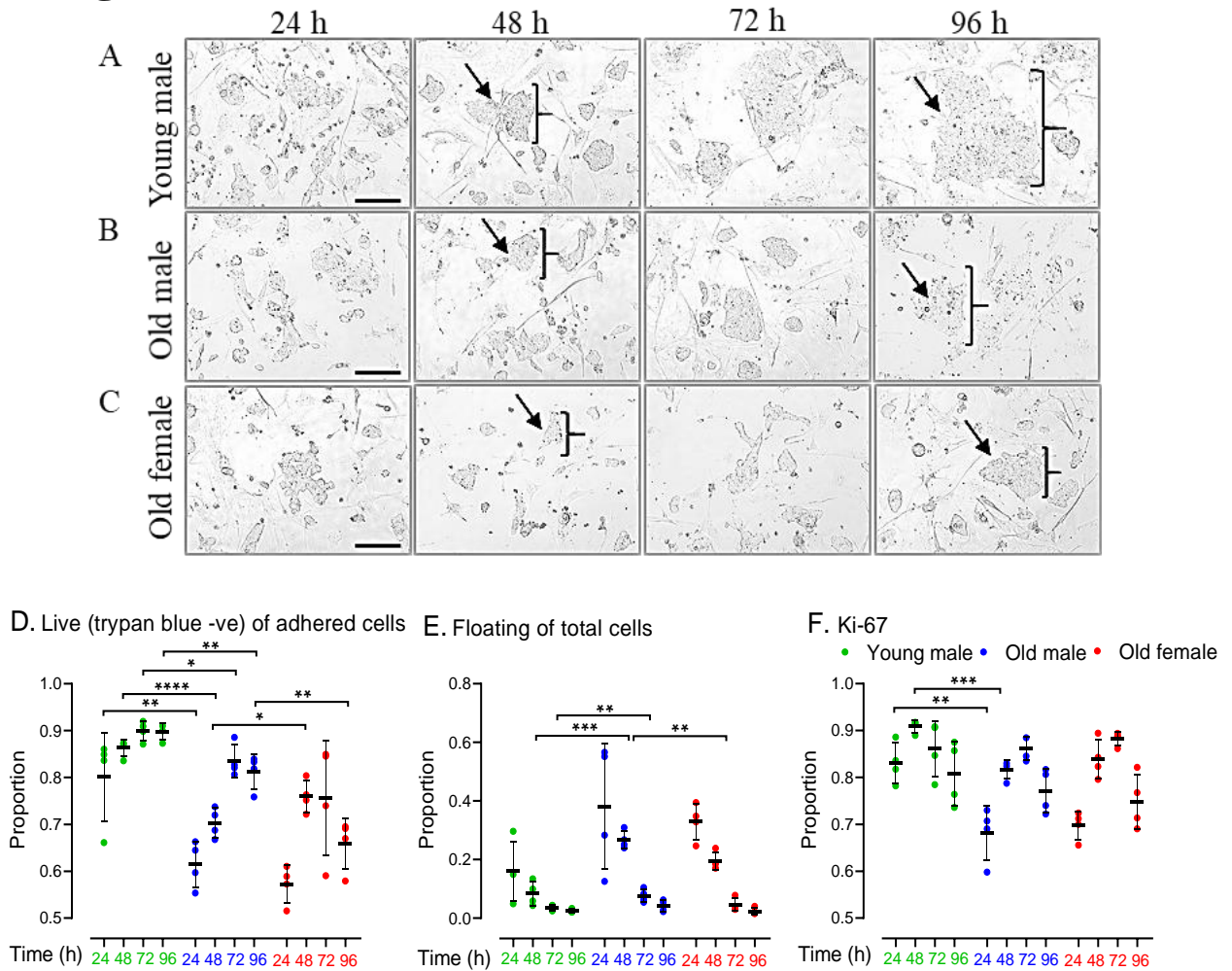


Figure 3. Cell proliferation and viability of undifferentiated Young male (7-8 weeks), Old (7-8 months) male, and female mESC lines. (A-C) Representative phase-contrast images of cell proliferation of Young male, Old male and Old female mESCs. After seeding, images were captured every 24 h over a period of 96 h. Images show that Young male (A) mESC lines have larger colonies with increased density of cells/ colony compared to Old male (B) mESC lines. Old Female mESC lines (C) present much smaller colony size and fewer mESC clones compared to Old Male mESC lines. Arrows and parenthesis point toward the colony size differences across the groups. Magnification = 100 μ m. (D, E) Trypan negative (live) cells are presented as proportion of adherent (live and dead) cells, and floating cells as proportion of total (live, dead and floating) cells. (D) Old male mESC lines had fewer live adherent cells at all time points, and (E) increased proportion of floating cells at 48 h and 72 h, as compared to Young male mESC lines. (F) Protein expression of cell proliferation marker Ki67 over time presented as the proportion positive of total cells (stained and unstained). Ki67 expression was lower in Old vs Young mESC lines at 24 h ($P=0.011$) and 48 h ($P=0.001$). Data presented as means \pm SDs based on $n = 4$ mESC lines per group. * $P<0.01$, ** $P<0.001$, *** $P<0.0001$, **** $P<0.00001$. Note: for (D-F), comparisons between Old Male and Young Male for ageing effects and between Old Male and Old Female for sex effects were normalised and analysed by t-test separately hence without post-hoc correction and placed in same chart for conciseness.

Figure 4

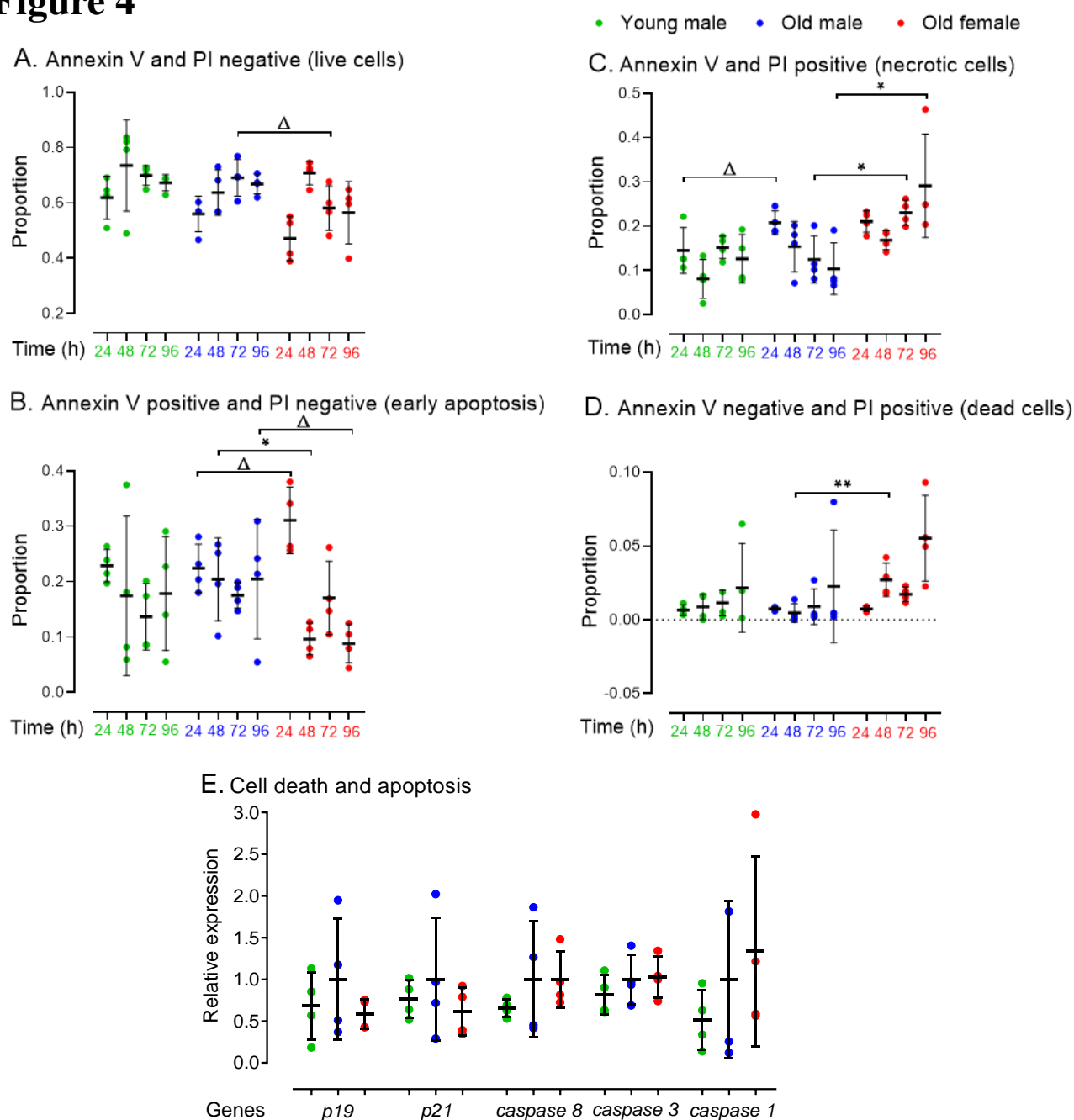


Figure 4. FACS analysis for detection of early apoptosis (Annexin V) and cell death (PI) in undifferentiated Young (7-8 weeks) vs Old (7-8 months) male, and Old male vs Old female (7-8 months) mESC lines. mESCs were cultured in duplicate. (A-D) Data is presented as proportion of total cells. Compared to the Young group, Old mESCs presented (C) increased necrosis at non-significant trend at 24 h ($P=0.075$) although the (B) proportion of early apoptotic cells was unaffected by age and time. Sex differences were observed within the Old mESC group where Old Female mESC lines showed (B) increased proportion of early apoptotic cells at non-significant trend ($P=0.059$) at 24 h, which decreased at 48 h ($P=0.055$) and 96 h ($P=0.085$) also at non-significant trend. Old Female mESC lines also exhibited increased proportion of (C) necrotic cells at 72 h ($P=0.035$) and 96 h ($P=0.035$), and (D) dead cells at 48 h ($P=0.01$) compared to Old male mESC lines. (E) However, RT-qPCR analysis of cell apoptotic markers was unaffected by maternal age and sex. Data presented as means \pm SDs based on $n = 4$ mESC lines per group, where Δ = trending $P < 0.1$, * = $P < 0.05$ and ** = $P < 0.01$. Note: for (A-E), comparisons between Old Male and Young Male for ageing effects and between Old Male and Old Female for sex effects were normalised and analysed by t-test separately hence without post-hoc correction and placed in same chart for conciseness.

Figure 5

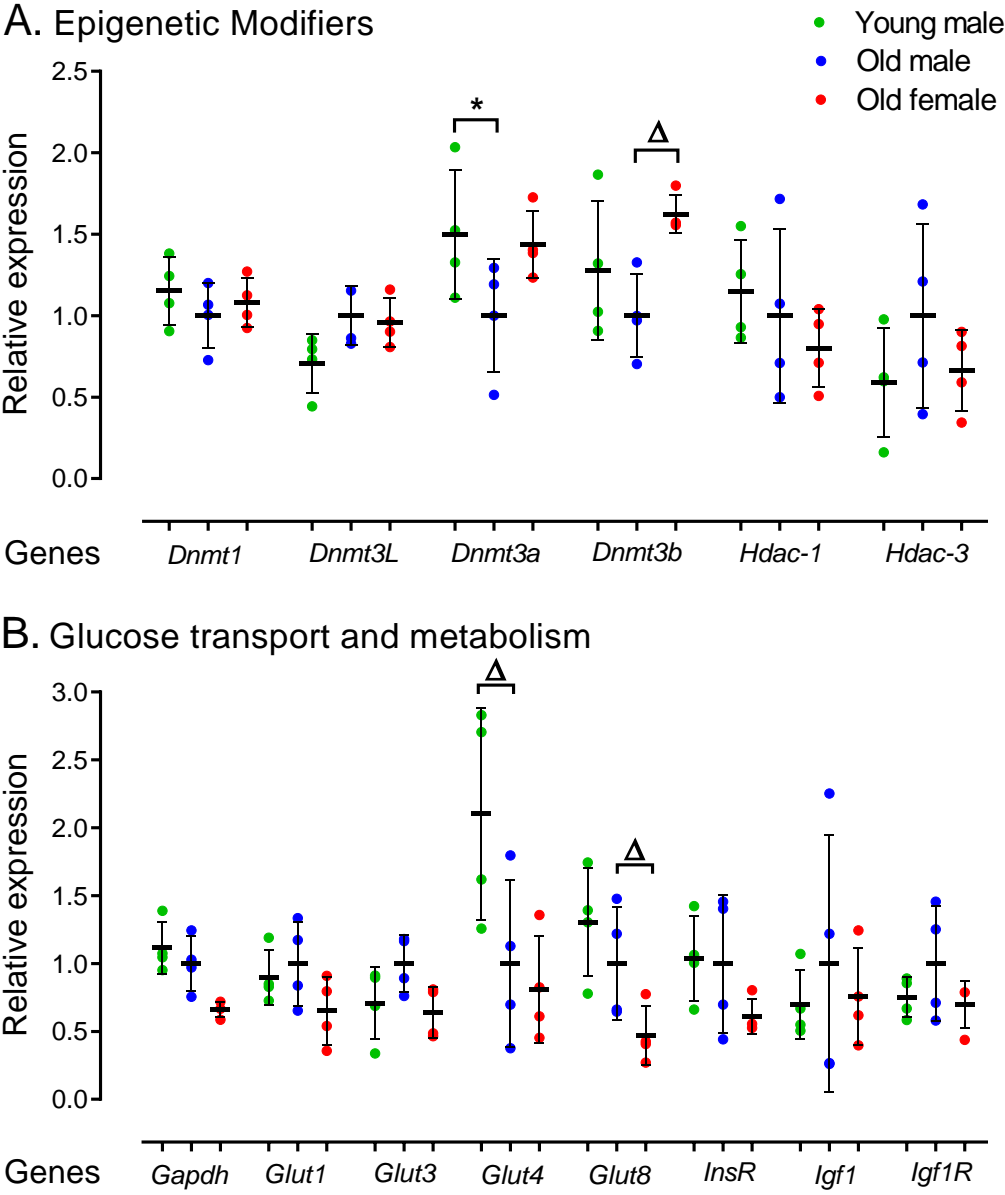


Figure 5. Relative gene expression for epigenetic modifiers and glucose transporters in undifferentiated Young (7-8 weeks) vs Old (7-8 months) male and Old male vs Old female (7-8 months) mESC lines. Real-time PCR analysis of DNA methyltransferases *Dnmt1*, *Dnmt3L*, *Dnmt3a* and *Dnmt3b*, histone modifiers *Hdac1* and *Hdac3*; glucose transporters *Glut1*, *Glut3*, *Glut4* and *Glut8* and metabolizers *Gapdh*, *InsR*, *Igf1* and *Igf1R*. Genes of interest were normalized to *Ywhaz* and *Rpl13a* within geNorm. (A, B) Old male mESC lines showed reduced expression of *Dnmt3a* ($P=0.049$) and *Glut4* at non-significant trend level ($P=0.0685$) compared to Young male mESC lines. Old Female mESC lines showed reduced expression of *Dnmt3b* at non-significant trend ($P=0.078$) and increased relative expression of *Gapdh* ($P=0.029$) and *Glut8* ($P=0.055$) at non-significant trend compared to Old Male mESC lines. Data presented as means \pm SDs based on $n = 4$ mESC lines per group. * indicates $P < 0.05$ and ^ indicates trend $P < 0.1$. Note: for (A,B), comparisons between Old Male and Young Male for ageing effects and between Old Male and Old Female for sex effects were normalised and analysed by t-test separately hence without post-hoc correction and placed in same chart for conciseness.